Proc. of the 9th Intl. Conf. of Asian Society for Precision Engg. and Nanotechnology (ASPEN 2022)
15–18 November 2022, Singapore. Edited by Nai Mui Ling Sharon and A. Senthil Kumar
doi://10.3850/978-981-18-6021-8_OR-09-0158

Tool point FRF estimation on multipurpose spindle by compensation of contact parameter

Jooho Hwang [1,#], Dang Chi Cong[1], Jongyoup Shim[1]

1 Department of Ultra-Precision Machines & Systems, Korea Institute of Machinery and Materials, 156, Gajeongbuk-Ro, Yuseong-Gu, Daejeon 34103, Republic of Korea
Corresponding Author / Email: jooho@kimm.re.kr, TEL: +82-42-868-7677, FAX: +81-868-7180

KEYWORDS: Spindle, Modeling, Stability, Drawbar, RCSA

Contact parameter in the high-speed spindle is an important parameter in tool point frequency response function (FRF) prediction, or receptance, which is the key factor in calculating the best operation condition of the spindle. In this paper, we describe an approach for the compensation tool and tool holder contact parameter by removing the effect of mass loading of an accelerometer used in the experiment process. The mass effect of the accelerometer is removed from tool point FRF by inversed Receptance Coupling Substructure Analysis (RCSA) in advance of estimating the contact parameter. The result contact parameter was used to predict the tool point FRF of the spindle. The drawbar in the automatic tool change mechanism is coupled to the shaft of the spindle. The contact parameter of a tool holder and tool is evaluated from the experiment. The tool, tool holder and shaft receptance were modeled by the Timoshenko beam theory. The fidelity of tool point FRF of spindle and stability lobe diagram after being predicted with the proposed method is improved.

1. Introduction

The high-speed spindle is used widely in industry. Its performance can be predicted by tool point FRF, which predicts a high-speed spindle in a stable or unstable condition. This can prevent spindle form running at critical speed, or chatter condition through stability lobe diagram [1,2].

Tool point FRF can be calculated using the RCSA method with the consideration of drawbar and contact parameter between shaft - tool holder and tool holder – tool connection [3], but the effect of accelerometer mass is not removed from experiment data. The accelerometer affects the result of the impact test by adding its mass to the spindle system. Kiran et al. [4] provided a method to remove the effect of accelerometer mass on the FRF of tool point. However, the contacting parameter was not mentioned. In the spindle design process, to get a better prediction of spindle dynamics, the database of the component dynamics and contact parameters should be well defined. The contact parameter was not evaluated in the in-depth process by missing the consideration of the drawbar or accelerometer mass [5]. The contact parameter of the shaft and tool holder is not considered frequently compared to the contact parameter of the tool holder and tool in predicting the tool point FRF.

In this paper, the contact parameter of the tool holder and tool was uncertificated using the inverse RCSA method firstly. The mass of the accelerometer is removed in advance of contact parameter evaluation. Secondly, we couple the drawbar to the shaft using a multiple-point coupling method. Then, the aerostatics bearing stiffness and shaft–tool holder contact parameter was evaluated. Finally, we used two contact parameters, which were evaluated in previous sections and the RCSA method to predict tool point FRF of the aerostatic spindle.

2. Inversed RCSA background

RCSA is a mathematical technique that predicts the assembly's receptance by coupling the component receptance. RCSA has the form in Equation (1), where H_{11} is assembly receptance and $h_{1a1a} = x_{1a1a}/f_{1a1a}$, $h_{1b1b} = x_{1b1b}/f_{1b1b}$ are component direct receptance[4].

$$H_{11} = h_{1a1a} - h_{1a1a}(h_{1a1a} + h_{1b1b})^{-1} h_{1a1a} \quad (1)$$

The inversed RCSA is derived from the RCSA technique. One component receptance, h_{1b1b}, is predicted by Equation (2a), with the condition of the other component receptance, h_{1a1a} and assembly receptance H_{11} are known [4].

$$h_{1b1b} = -h_{1a1a} + h_{1a1a}(h_{1a1a} - H_{11})^{-1} h_{1a1a} \quad (2a)$$

In the experiment, the accelerometer (h_{1a1a}) is considered to coupling with the spindle system at tooltip forming an assembly (H_{11}) of spindle system and accelerometer. The effect of accelerometer mass (h_{1a1a}) should be removed from measured assembly FRF (H_{11}) as in Equation (2b) as in (rad/s) [4,6]

$$[\mathbf{h_{1a1a}}] = \frac{\mathbf{x_{1a}}}{\mathbf{f_{1a}}} = -\frac{\mathbf{1}}{\mathbf{m\omega^2}} \quad (2b)$$

3. Contact parameter estimation

In the spindle system, there are several contact parameters including shaft-tool holder and tool holder-tool contact parameter. The compensation process is applied for tool holder-tool contact parameter and is not the shaft-tool holder contact parameter. The reason is due to the effect of accelerometer mass on shaft-tool holder contact parameter is trivial.

The tool point FRF is estimated as in equation (3)

$$[G_{11}] = R_{11} - R_{12a}(R_{2a2a}+R_{2b2b}+[K]^{-1})^{-1}R_{2a1} \qquad (3)$$

$[G_{11}]$ is the dynamic response of the assembly at point 1 of spindle in Figure 1. Rij is the generalized component receptance matrix. The contact parameter has the form of a matrix of complex number as in Equation (4):

$$[\mathbf{K_a}]=\begin{bmatrix} k_{xf}+i\omega c_{xf} & k_{xm}+i\omega c_{xm} \\ k_{\theta f}+i\omega c_{\theta f} & k_{\theta m}+i\omega c_{\theta m} \end{bmatrix} \qquad (4)$$

These include four types of stiffness, relating to the transverse displacement to force k_{xf}, displacement to moment k_{xm}, rotation to force $k_{\theta f}$, rotation-to-moment stiffness $k_{\theta m}$, and four types of damping, namely displacement to force c_{xf}, displacement to moment c_{xm}, rotation to force $c_{\theta f}$, and rotation-to-moment damping $c_{\theta m}$; ω is the frequency.

The tool holder-tool contact parameter is denoted as $[K_{2\_1}]$ and is estimated by Equation (5):

$$[\mathbf{K}_{2\_1}]=\left(\left([\mathbf{R}_{12a}]^{-1}([\mathbf{R}_{11}]-[\mathbf{G}_{11}])[\mathbf{R}_{2a1}]^{-1}\right)^{-1}-[\mathbf{R}_{2a2a}]-[\mathbf{G}_{2b2b}]\right)^{-1} \qquad (5)$$

$[G_{ii}]$ is the dynamic response of the assembly at point i. Rij is the generalized component receptance matrix of a 33.5mm overhang tool, including the translational and rotational motion [7] of the tool as shown in Figure 1. Rij is calculated by the Timoshenko beam theory.

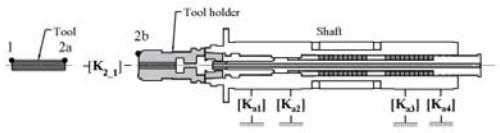

Fig. 1 Tool holder - tool contact parameter estimation

In Equation (5), The contact parameter $[K_{2\_1}]$ between the tool holder and tool can be calculated by rearranging Equation (3) as in [8], where one value of the contact parameter was chosen for each corresponding tool holder mode frequency from a set of contact parameters calculated using Equation (4) over the desired frequency range. However, in reality, the effect of the accelerometer should be removed from measured data before obtaining the exact G_{11}. The receptance G_{11} is described in equation (6):

$$[\mathbf{G_{11}}]=\begin{bmatrix} \frac{X_1}{F_1} & \frac{X_1}{M_1} \\ \frac{\Theta_1}{F_1} & \frac{\Theta_1}{M_1} \end{bmatrix}=\begin{bmatrix} H_{11}^{true} & L_{11}^{true} \\ N_{11}^{true} & P_{11}^{true} \end{bmatrix} \qquad (6)$$

where X_{2b} and Θ_{2b} are the transverse deflection and rotation at point 2b, respectively; F_{2b} and M_{2b} are the force and moment at point 2b, respectively. $H_{11} = X_1/F_1$ is measured and the other receptances L^{true}_{11}, N^{true}_{11}, P^{true}_{11} are obtained through the technique stated in [9].

We used a tool holder with 27.5 mm collet length in this experimental setup. The carbide blank tool with 32.5mm overhang length and 6mm diameter was clamped to the tool holder of the spindle and the spindle was placed on foam to represent the free-free boundary condition. All the tools used in this paper have diameter of 6mm. The measured data of tool point FRF, H_{11} and calculated data of tool point FRF, $H^{updated}_{11}$ after removing the effect of mass loading the effect of the accelerometer are displayed in Figure 2. The accelerometer mass is 0.6 grams.

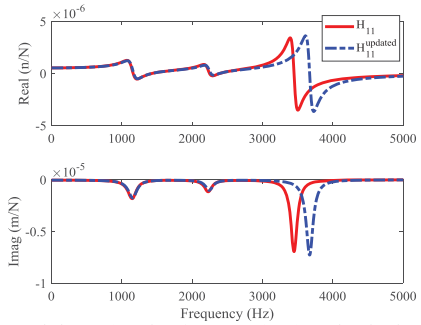

Fig. 2 Measured data of tool point FRF (H_{11}) and calculated data of tool point FRF ($H^{updated}_{11}$) after removing the mass effect

The assembly receptance G_{11} is obtained by the method mentioned in the previous paragraph. The contact parameter between tool holder and tool is consequently calculated by Equation 5 and stated in Table 1.

4. Tool point FRF and stability lobe diagram prediction

The whole spindle system is modeled as described in [3]. The effect of drawbar is also taken into account. A drawbar has a common neutral axis and is located inside a shaft. We used the four-point receptance coupling approach to describe the dynamic response of the combination of shaft and drawbar, as in [10]. These four points denoted as c1, c2, c3, c4 are the actual contact positions of the drawbar and the shaft; the structure is divided into three segments.

$$[\mathbf{G_{3b3b}}]=\frac{\mathbf{U_{c1}}}{\mathbf{Q_{c1}}}=\mathbf{R_{c1c1}}\frac{\mathbf{q_{c1}}}{\mathbf{Q_{c1}}}+\mathbf{R_{c1c2}}\frac{\mathbf{q_{c2}}}{\mathbf{Q_{c1}}}+\mathbf{R_{c1c3}}\frac{\mathbf{q_{c3}}}{\mathbf{Q_{c1}}}+\mathbf{R_{c1c4}}\frac{\mathbf{q_{c4}}}{\mathbf{Q_{c1}}} \qquad (7)$$

where $[G_{3b3b}]$ is the dynamic response of the assembly of Substructure III at point 3b. R_{c1c1}, R_{c1c2}, R_{c1c3}, R_{c1c4} are the generalized component receptance matrix. q_j is the force vector including the force and moment acting on the drawbar. U_{c1} and Q_{c1} are the corresponding generalized displacement/rotation and external force/moment vectors acting on the shaft drawbar assembly, as shown in Fig. 3. The direct receptance of the shaft is represented as a Timoshenko beam model with aerostatic bearing dynamics $[K_{a1}]$, $[K_{a2}]$, $[K_{a3}]$, and $[K_{a4}]$; these were evaluated experimentally. The receptance of the drawbar was modeled as a Timoshenko beam model. After taking into account the effects of the drawbar, we modeled the arbitrary tool-holder receptance using Timoshenko beam theory, and then coupled it to the receptance of the shaft-drawbar assembly using Equation (8)

Table 1. Contact parameter of $[K_{2\_1}]$ in with and without accelerometer mass effect

	k_{xf} N/m	c_{xf} Ns/m	k_{xm} Nm/m	c_{xm} Nms/m	$k_{\theta f}$ N/rad	$c_{\theta f}$ Ns/rad	$k_{\theta m}$ Nm/rad	$c_{\theta m}$ Nms/rad
$[K_{2\_1}]$	6.95×10^{6}	1.38×10^{1}	1.52×10^{5}	0.29×10^{0}	1.52×10^{5}	0.29×10^{0}	2.33×10^{3}	0.07×10^{-1}
$[K_{2\_1}]_{true}$	1.09×10^{7}	3.87×10^{1}	2.33×10^{5}	0.80×10^{0}	2.33×10^{5}	0.35×10^{0}	4.10×10^{3}	0.17×10^{-1}

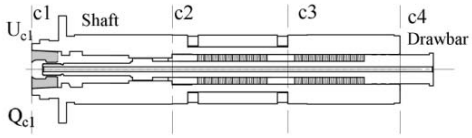

Fig. 3 Receptance coupling substructure analysis of the shaft and drawbar using four-point receptance coupling approach

$$[\mathbf{G_{2b2b}}]=[\mathbf{R_{2b2b}}]-[\mathbf{R_{2b3a}}]([\mathbf{R_{3a3a}}]+[\mathbf{G_{3b3b}}]+[\mathbf{K_{3\_2}}]^{-1})^{-1}[\mathbf{R_{3a2b}}] \quad (8)$$

Where $[K_{3\_2}]$ is the contact parameter between shaft- drawbar and tool holder. The contact parameter $[K_{3\_2}]$ is estimated in the same manner as $[K_{2\_1}]$ as stated in Section 3. The difference is that the assembly is not tool – tool holder – shaft – drawbar, but the assembly is tool holder – shaft – drawbar. The effect of acceleromter is not clear in this estimation process, therefore we can apply directly Equqtion 5, without demanding of removement of accelerometer mass effect. We then estimated the receptance based on our experimental results and the known value of the tool holder receptance.

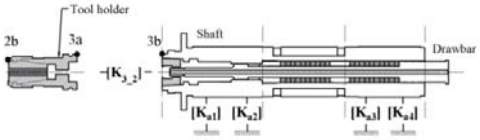

Fig. 4 Models of the spindle supported by aerostatic bearings using RCSA method

The next step was to couple the tool to the drawbar-shaft-tool holder assembly using Equation (9). The tool was modeled as a two-segment cylinder using the Timoshenko beam theory. The parameter $[K_{2\_1}]$ is the contact parameter between tool and tool holder which are provided in Section 3.

$$[\mathbf{G_{11}}]=[\mathbf{R_{11}}]-[\mathbf{R_{12a}}]([\mathbf{R_{2a2a}}]+[\mathbf{G_{2b2b}}]+[\mathbf{K_{2\_1}}]^{-1})^{-1}[\mathbf{R_{2a1}}] \quad (9)$$

The aerostatic spindle used in this study contained four bearings, $[K_{a1}]$, $[K_{a2}]$, $[K_{a3}]$, and $[K_{a4}]$. We assumed that the individual bearings in the front and rear sets were equal, i.e., $[K_{a1}] = [K_{a2}]$, $[K_{a3}] = [K_{a4}]$. These aerostatic bearing dynamics are estimated by turning their initial value until receptance calculated by Equation (8) was equal to measured receptance at point 2b.

Until this process, the tool point FRF can be calculated by Equation (9). As shown in Figure (5), both data are calculated one. The updated data is obtained by using the contact parameter without effect of accelerometer mass. In the original version of tool point FRF, natural frequencies (NF) are 1116 Hz, 2177 Hz and 3031 Hz. In the updated version of tool point FRF, NFs are 1118, 2187 Hz and 3152 Hz. The updated third NF differs 3.9% from the original version. This is important information for high-speed spindle design process.

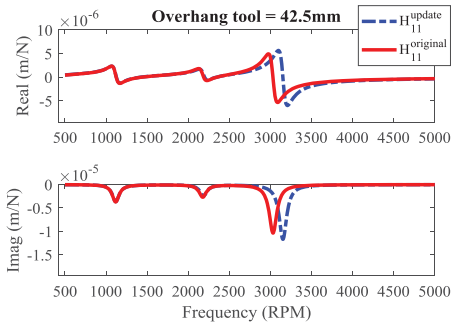

Fig. 5 Predicted tool point FRF for 42.5 mm overhang tool with accelerometer mass effect (red line) and without accelerometer mass effect (blue dash line)

The tool point FRF of 22.5 overhang tool is also estimated and the effect of the accelerometer is similar to the 42.5 mm overhang tool as shown in Figure (6). As shown in Figure (6), in the original version of tool point FRF, natural frequencies (NF) are 1135 Hz, 2217 Hz, and 3530 Hz. In the updated version of tool point FRF, NFs are 1138, 2223 Hz, and 3733 Hz. The updated third NF differs 5.7% from the original version. The shorter the overhang length of the tool is, the more the accelerometer mass affects on tool point FRF. In both cases of overhang tool, after the effect of mass is removed, the captured data belongs to merely the spindle system, not the spindle and the accelerometer themself; therefore, the mass of system related to updated data is decreased. Consequently, the natural frequency of the tooltip without the effect of accelerometer mass is larger than that with the effect of accelerometer mass.

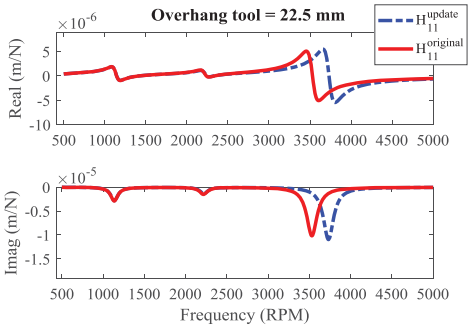

Fig. 5 Predicted tool point FRF for 22.5 mm overhang tool with accelerometer mass effect (red line) and without accelerometer mass effect (blue dash line)

The 42.5 mm overhang tool was chosen to estimate the stability lobe diagram. We estimated the stability lobe diagram (SLD) based on the FRF of the aerostatic spindle with the 42.5 mm tool as in one assumed condition. The SLDs of the FRF were calculated for three

different cases and the results are shown in Figure 7. We calculated the stability based on the FRF without the accelerometer effect and found it to be much improved concerning the depth of cut and spindle speed. These improvements did not only apply to low-speed operation (Fig. 7) but were also observed in the case of high-speed operation (Fig. 8). In high-speed operation, the error of 6% is increased from the original case.

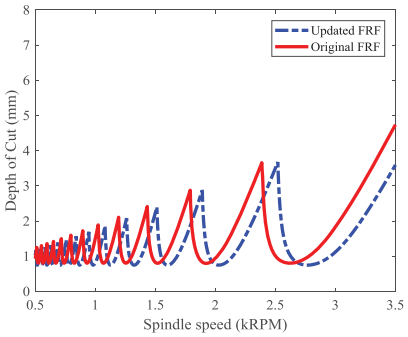

Fig. 7 Comparison between the results of the calculation with original FRF and updated FRF over the stability lobe diagram at low spindle speeds

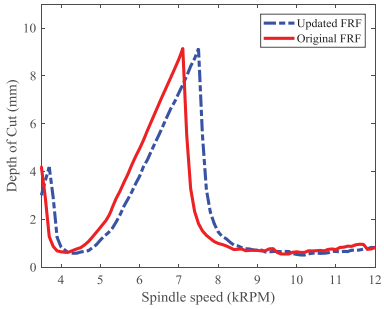

Fig. 8 Comparison between the results of the calculation with original FRF and updated FRF over the stability lobe diagram at high spindle speed

5. Conclusion

In this paper, we presented an updated method in predicting the tool point FRF of a multipurpose aerostatic spindle. By removing the effect of accelerometer mass, the tool point FRF measurement result and the contact parameter were updated in advance of the tool point FRF prediction method. The spindle system was modeled while considering the effect of the drawbar, the shaft, the aerostatic bearing, the tool holder, the shaft and tool holder contact parameter, and the updated tool and tool holder contact parameter using RCSA method. The drawbar is considered to be nested inside the shaft and model using multiple coupling method. The result of the predicted tool point FRF method is based on two methods including removing accelerometer mass effect and RCSA; therefore, we believed in the fidelity of predicted result. This paper combined the accelerometer mass effect elimination with the latest model of considering drawbar in spindle dynamics estimation; this could help the spindle designer have a better viewpoint of spindle dynamics from the beginning design process.

REFERENCES

1. Tlusty, J. *Manufacturing Processes and Equipment*, Prentice Hall, Upper Saddle River, NJ, 2000.
2. Budak, E., Altintaş, Y., “Analytical Prediction of Chatter Stability in Milling—Part I: General Formulation,” J. Dyn. Syst. Meas. Control. . Vol. 120, pp. 22-30, 1998.
3. Cong, D.C. , Hwang, J., Shim, J., Ro, S.K., Schmitz, T., “,” Int. J. Mach. Tools Manuf. Vol.144 pp. 103424, 2019.
4. Kiran, K., Satyanarayana, H., Schmitz, T., “Compensation of frequency response function measurements by inverse RCSA”, Int. J. Mach. Tools Manuf., Vol. 121, pp. 96-100, 2017.
5. Ertürk, A., Özgüven, H.N., Budak, E., “Analytical modeling of spindle-tool dynamics on machine tools using Timoshenko beam model and receptance coupling for the prediction of tool point FRF,” Int. J. Mach. Tools Manuf. Vol. 46, pp.1901-1912, 2006.